Conformational Control of Thymine Photodimerization in Single-Strand and Duplex DNA Containing Locked Nucleic Acid TT Steps

ARTICLE *in* JOURNAL OF THE AMERICAN CHEMICAL SOCIETY · OCTOBER 2010

Impact Factor: 12.11 · DOI: 10.1021/ja108528q · Source: PubMed

J|A|C|S COMMUNICATIONS

Published on Web 08/25/2010

Conformational Control of Thymine Photodimerization in Single-Strand and Duplex DNA Containing Locked Nucleic Acid TT Steps

Mahesh Hariharan,[†,‡] Martin McCullagh,[†] George C. Schatz,[†] and Frederick D. Lewis*[,†]

Department of Chemistry, Northwestern University, Evanston, Illinois 60208-3113, and School of Chemistry, Indian Institute of Science Education and Research Thiruvananthapuram, Kerala, India 695016

Received July 13, 2010; E-mail: fdl@northwestern.edu

Abstract: The results of an integrated experimental and theoretical study of thymine−thymine photodimerization in short single-strand and duplex DNA structures possessing a single locked nucleic acid TT step are reported. Control of ground-state conformation by the locked nucleic acids results in a marked increase in both the quantum yield and the selectivity of photoproduct formation.

Dimerization of adjacent thymines in DNA is a leading cause of damage to cellular DNA by UV light.[1] The possibility that the products and efficiency of thymine dimerization are related to ground-state conformation as well as base sequence was first suggested over 40 years ago.[2] Conformational control of dimerization efficiency requires that photodimerization be more rapid than equilibration of reactive and nonreactive excited-state conformations (Scheme 1).[3] Recently, experimental evidence for ultrafast TT dimerization based on femtosecond time-resolved IR spectroscopy was presented by Gilch and co-workers for the oligonucleotide $(dT)_{18}$ and the dinucleotides TT and T_LT_L, where T_L is the locked nucleic acid analogue of dT in which the furanose ring is locked in the C3′-endo conformation.[4] Ultrafast TT dimerization is also consistent with recent theoretical studies that show barrier-free entry into the conical intersection for photodimerization.[5,6] A recent report of higher dimerization efficiency and selectivity for formation of the major (2+2) dimer from T_LT_L vs TT provides additional evidence for conformational control of TT dimerization in dinucleotides.[7] However, this intriguing observation has not been extended to the more biologically relevant single-strand or duplex systems.

Scheme 1. Schematic Representation of Unreactive (A) and Reactive (B) Conformations for TT Steps in Single-Stranded DNA and a Reaction Scheme for Thymine (2+2) Dimerization

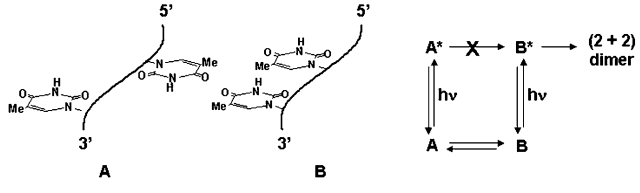

In spite of the ultrafast character of TT dimerization, reaction efficiencies are low for single-strand poly(dT) ($\Phi = 0.05$) and even lower for cellular DNA ($\Phi = 10^{-3}$).[8] Molecular modeling of the ground-state conformations of $(dT)_2$ by Law et al.[9] and $(dT)_{18}$ by Johnson et al.[10] led to the proposal of models similar to those for solid-state dimerization[11] for conformational control of TT dimerization based on the distance and dihedral angle between double bonds in which the ground-state populations of reactive conformers were small. A simpler theoretical model presented by McCullagh et al.[6] based only on distance was found to correctly describe trends in both (2+2) and (6−4) dimerization efficiency for the duplex $(dT)_{20}(dA)_{20}$ as well as $(dT)_{20}$ and for several alkane-linked mini-hairpins possessing a single TT step at different locations within the base-pair stem.

We report here a combined experimental and theoretical investigation of the efficiency and products of TT photodimerization in the dinucleotide **1L**, in the single-strand oligonucleotide **2L** which contains a locked nucleic acid (LNA) T_LT_L step, and in the alkane-linked hairpins **3L**−**7L** which possess only A-T base pairs and a single T_LT_L step (Chart 1). The results are compared to those recently reported for the same structures possessing a normal TT step.[12] We find a remarkable increase in the quantum yield of thymine dimer formation in T_LT_L vs TT steps in single-strands **1** and **2**, in hairpin overhangs **3** and **4**, and in the nonlinked end of hairpin **5**. In contrast, the increases in quantum yield for T_LT_L vs TT steps within the base-paired duplex domains of **6** and **7** are relatively modest. Our computational model for TT dimerization replicates the experimental trends and provides a rationale for the more pronounced sensitivity of single-strand vs duplex structures to the replacement of a TT step by T_LT_L.

Chart 1. Structures of (a) TT (2+2) Dimer, (6−4) Adduct, C12 Linker, and Locked Nucleic Acid T_L and (b) Dinucleotide **1L**, Single-Strand Oligo **2L**, and C12-Linked Hairpins **3L**−**7L** Containing an LNA T_LT_L Step; Corresponding Sequences with Unmodified TT Steps Are Designated **1**−**7**

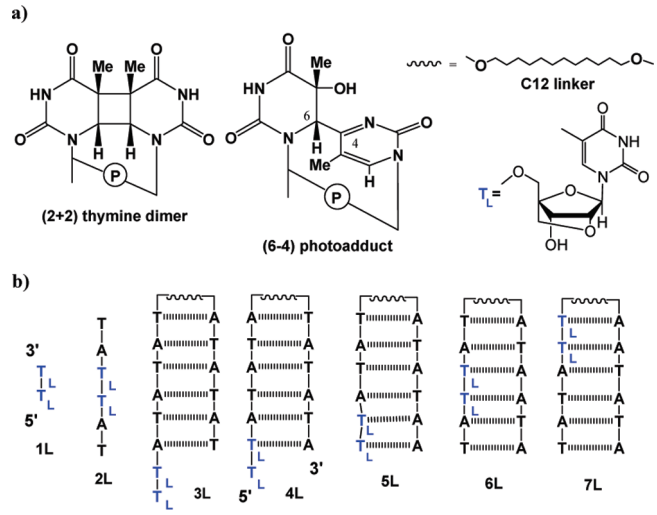

Oligonucleotide conjugates containing T_LT_L steps (Chart 1) were prepared and characterized as described in the Supporting Information. The UV and CD spectra of these conjugates are similar to

[†] Northwestern University.
[‡] Indian Institute of Science Education and Research Thiruvananthapuram.

10.1021/ja106203q

those of the analogous conjugate possessing a TT step, as shown for **7L** vs **7** in Figure S1 (Supporting Information). Melting temperatures for **3L**−**7L** in 10 mM phosphate buffer (pH 7.2) containing 100 mM sodium chloride are higher than for hairpins possessing TT steps (Table S2, Supporting Information), as reported for incorporation of one or more T_L base into DNA duplexes.[13]

Solutions containing ca. 1−1.2 μM hairpin in phosphate buffer were irradiated with monochromatic 280 nm light at 10 °C in 1 cm path length quartz cuvettes. The progress of irradiation was monitored by high-temperature HPLC, with a detection wavelength of 260 nm and a column temperature of 60 °C. The long-wavelength absorption band of **1L** is completely bleached upon irradiation, whereas the bands of the other conjugates are reduced in intensity but little changed in band shape. The growth of a single product peak having a shorter retention time than the starting material is observed for **1L**−**7L**. Representative HPLC traces obtained at 10 min irradiation intervals for hairpin **7L** are shown in Figure S2 (Supporting Information). The products peaks have the same mass as the starting materials and undergo reversion to starting materials upon irradiation at 240[14] or 254 nm,[15] as expected for (2+2) thymine dimer. The (6−4) adducts previously observed as minor products upon irradiation of **1** and **7** are not observed in the cases of **1L** and **7L**. The isolated product from hairpin **7L** has a value of T_M = 56.4 °C, lower than that of **7L** (60.6 °C). The resulting change in T_M (ΔT_M = 4.2 °C) is smaller than that for the dimer of **7** (ΔT_M = 15.4 °C), indicative of enhanced stability for the (2+2) dimer as well as for the starting material possessing a T_LT_L vs TT step.

Plots of T_LT_L dimerization vs irradiation time for **1L**, **2L**, and **6L** and their unmodified analogues are shown in Figure 1. In all three cases, product formation is more rapid for the LNA-containing sequences. The high conversions obtained for **1L** and **2L** are consistent with clean conversion to a single adduct that does not absorb appreciably at 280 nm. Relative quantum yields obtained from the initial slopes of these plots are converted to absolute quantum yields by the method previously described for TT-containing hairpins.[6] Quantum yields for (2+2) dimerization of **1L**−**7L** and **1**−**7** and the ratios of these quantum yields are reported in Table 1. Values for **2L**−**7L** and **2**−**7** are not corrected for competitive absorption by nonreactive bases and would be higher if such corrections were made. Our values for **1L** and **1** and their ratio are similar to those obtained by Desnous et al. using 254 nm irradiation.[7] Quantum yields for TT dimerization are known to be wavelength dependent.[16] Even larger enhancements of the quantum yields for T_LT_L vs TT dimerization are observed for single-stranded oligo **2L**, for hairpins **3L** and **4L** (which possess double or single T_L overhangs, respectively), and for hairpin **5L** (which has a T_LT_L step at the nonlinked end of the hairpin). A more modest increase in quantum yield is observed for a T_LT_L vs TT step in the interior or adjacent to the linker of hairpins **6L** and **7L**.

Conformational modeling of **1L**, **2L**, and **5L**−**7L** was carried out using the CHARMM[17] force field with the addition of the locked nucleic acid parameters from Pande et al.[18] as described in the Supporting Information. Probability densities for the distance d separating the midpoints of the T_LT_L C5−C6 double bonds in **1L**, **2L**, and **6L** are shown in Figure 2, along with results for the unmodified sequences. Significantly narrower distributions of d were seen for all of the locked systems in comparison to the nonlocked systems, the difference being more pronounced for **1L** and **2L** than for **6L**. The peak in the probability density for the sequences **1L** and **2L** lies at shorter distances (ca. 3.8 and 4.0 Å) as compared to the 4.2 Å separation in hairpin **6L**. Narrower distributions of the C5−C6−C6′−C5′ dihedral angle, η, were also observed for the

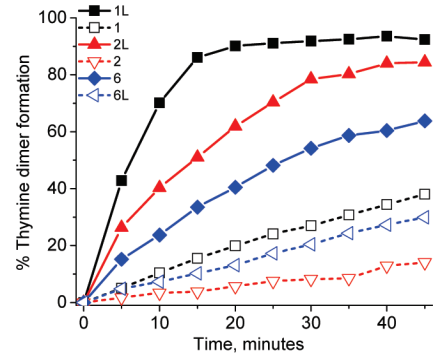

Figure 1. Relative percentage thymine dimer formation of sequences **1L**, **2L**, and **6L** vs **1**, **2**, and **6** as determined using HPLC with increasing time of irradiation at 280 nm as monitored at 260 nm.

Table 1. TT Dimerization Quantum Yields for LNA T_LT_L-Containing Sequences **1L**−**7L** and Unmodified TT-Containing Sequences **1**−**7**

	1	**2**	**3**	**4**	**5**	**6**	**7**
$10^{-3}\Phi_{TT}$	0.95	0.40	0.39	0.38	0.39	0.92	1.1
$10^{-3}\Phi_{T_LT_L}$	8.3	6.1	7.4	7.9	4.1	3.4	4.4
$\Phi_{T_LT_L}/\Phi_{TT}$	9	15	19	20	11	4	4

locked vs unmodified TT steps (Figures S4 and S5, Supporting Information).

TT dimerization quantum yields were calculated using the single criterion d < 3.52 Å obtained in our previous study, using the dimerization quantum yields for $(dT)_{20}$ and $(dT)_{20}(dA)_{20}$ as benchmarks.[6] Conformations that meet this criterion also have restricted values of the dihedral angle η, making a second criterion unnecessary. Quantum yields determined by this procedure are reported in Table 2. The calculated values for the ratios of T_LT_L vs TT dimerization replicate the important trends in the experimental data, namely the large ratios for **1**, **2**, and **5** and the much smaller ratios for **6** and **7**. Calculated quantum yields for the formation of (6−4) adducts reported in Table S3 (Supporting Information) are very low ($\leq 0.5 \times 10^{-3}$) for all of the T_LT_L and TT sequences investigated except **7**, in agreement with the experimental results.

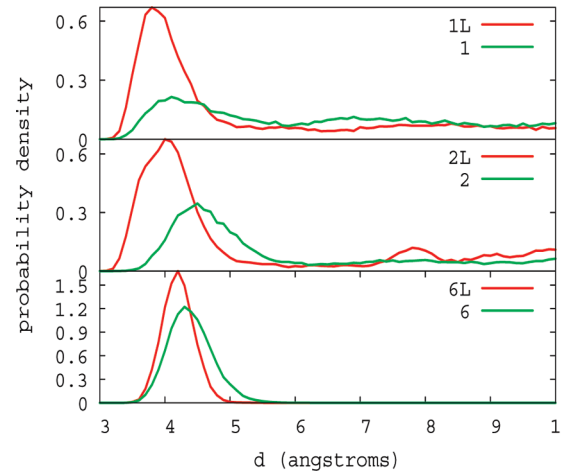

Figure 2. Probability densities for the C5−C6 bond separation for T_LT_L (red lines) vs TT steps (green lines) in (top) **1D** vs **1**, (middle) **2L** vs **2**, and (bottom) **6D** vs **6**. The integral of the population density is 1.0.

Randomly selected snapshots of reactive conformations of **1L**, **2L**, and **6L** and their unmodified analogues are shown in Figure 3. Differences between the locked and nonlocked structures become

Table 2. Quantum Yields for TT Dimerization from MD Simulations Calculated with the Cutoff of $d < 3.52$ Å for LNA T_LT_L-Containing Sequences **1L**, **2L**, and **5L**−**7L** and Unmodified TT-Containing Sequences **1**, **2**, and **5**−**7**

	1	2	5	6	7
$10^{-3}\Phi_{TT}$	9	2.3	1.5	1.5	0.9
$10^{-3}\Phi_{T_LT_L}$	62	77	31.7	1.8	2.5
$\Phi_{T_LT_L}/\Phi_{TT}$	6.9	33	21	1.2	2.8

evident upon analysis of probability distributions of helical parameters (rise, shift, slide, tilt, roll, and twist) between adjacent thymines (Figures S4 and S5). The T_LT_L steps for **1L** and **1** (Figure S4) and for **2L** vs **2** (Figure S5) sample a much narrower range of values than the nonlocked. Differences in the structures of **6L** and **6** (Figure 3E,F) are more obvious and include larger buckle angles for T_L-A (−8° and −16°; nearest to the 5′ end) than for the corresponding T-A base pairs (0° and −4°) (Figure S6, Supporting Information). Similar large buckle angles are observed in the NMR structure of a 10-base-pair duplex having a T_LT_L step at midstrand.[19] Smaller differences are calculated for the propeller angle and opening angle (Figure S6) and the rise, roll, twist, and tilt distributions (Figure S5) for the T_LT_L vs TT steps of **6L** vs **6**. The A-T base pairs adjacent to the T_LT_L step in **6L** appear to have normal B-DNA geometries, in accord with previous NMR,[19] X-ray crystal structure,[20] and molecular dynamics studies[17,18] which show that the structural perturbation introduced by a single locked nucleotide is localized.[21]

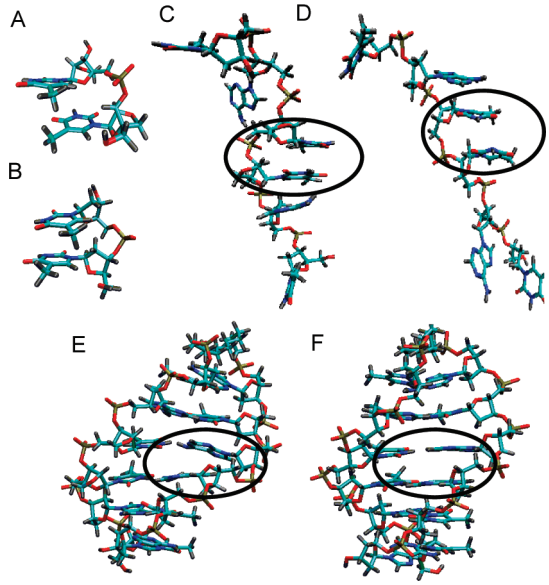

Figure 3. Snapshots of TT stacked conformations from molecular dynamics simulations of (A) **1L**, (B) **1**, (C) **2L**, (D) **2**, (E) **6L**, and (F) **6**. Ovals indicate the location of the TT step in structures C−F.

In summary, we observe increases in the quantum yields for dimerization at T_LT_L vs TT steps in a single-strand and hairpin overhangs (Table 1) which are even larger than those previously reported by Desnous et al.[7] for the dinucleotides. Molecular dynamics simulations indicate that the increased quantum yield for the single-strand sequence **2L** is a consequence of a marked increase in the population of ground-state conformations having geometries appropriate for dimerization of T_LT_L vs TT steps (Scheme 1A). More modest increases in quantum yields are observed for the T_LT_L vs TT steps in hairpins **6L** and **7L** (Table 1). Molecular dynamics simulations indicate that the more rigid duplex structure of hairpin **6L** prevents the close approach of the reactive double bonds observed in **1L** and **2L** and thus allows only a minor increase in the population of reactive conformations for the T_LT_L vs TT step (Figure 2). Presumably the populations of reactive conformations in the single and double overhang sequences **3L** and **4L**, which also show large increases in quantum yield, are similar to those in single-strand sequences. The increase in quantum yield for **5L** vs **5** is intermediate between those for the duplex interior (**6L** vs **6**) and for the single and double overhangs, suggestive of intermediate conformational populations for a terminal T_LT_L step. The more rigid structures of the T_LT_L vs TT steps are inappropriate for the formation of (6−4) adducts or other minor TT photoadducts, resulting in highly selective formation of the syn (2+2) photoadducts. These results serve to elucidate the photochemical behavior of T_LT_L steps in single-strand and duplex DNA and to further establish the importance of ground-state conformation in determining the efficiency and selectivity of TT dimerization, particularly in single-strand sequences.

Acknowledgment. Funding for this project was provided by the National Science Foundation (NSF-CRC grant CHE-0628130).

Supporting Information Available: Experimental Section and relative percent dimer formation of **1L**−**7L** and **1**−**7**; probability density plots for **1L**, **2L**, and **6L** in comparison with **1**, **2**, and **6**, respectively. This material is available free of charge via the Internet at http://pubs.acs.org.

References

(1) (a) Beukers, R.; Berends, W. *Biochim. Biophys. Acta* **1960**, *41*, 550. (b) Beukers, R.; Eker, A. P. M.; Lohman, P. H. M. *DNA Repair* **2008**, *7*, 530. (c) Setlow, R. B. *Science* **1966**, *153*, 379. (d) Taylor, J. S.; Brockie, I. R.; O'Day, C. L. *J. Am. Chem. Soc.* **1987**, *109*, 6735.
(2) (a) Kleopfer, R.; Morrison, H. *J. Am. Chem. Soc.* **1972**, *94*, 255. (b) Becker, M. M.; Wang, J. C. *Nature* **1984**, *309*, 682. (c) Becker, M. M.; Wang, Z. *J. Mol. Biol.* **1989**, *210*, 429.
(3) Schreier, W. J.; Schrader, T. E.; Koller, F. O.; Gilch, P.; Crespo-Hernandez, C. E.; Swaminathan, V. N.; Carell, T.; Zinth, W.; Kohler, B. *Science* **2007**, *315*, 625.
(4) Schreier, W. J.; Kubon, J.; Regner, N.; Haiser, K.; Schrader, T. E.; Zinth, W.; Clivio, P.; Gilch, P. *J. Am. Chem. Soc.* **2009**, *131*, 5038.
(5) (a) Boggio-Pasqua, M.; Groenhof, G.; Schaefer, L. V.; Grubmueller, H.; Robb, M. A. *J. Am. Chem. Soc.* **2007**, *129*, 10996. (b) Blancafort, L.; Migani, A. J. *Am. Chem. Soc.* **2007**, *129*, 14540.
(6) McCullagh, M.; Hariharan, M.; Lewis, F. D.; Markovitsi, D.; Douki, T.; Schatz, G. C. *J. Phys. Chem. B* **2010**, *114*, 5215.
(7) Desnous, C.; Babu, B. R.; Moriou, C.; Mayo, J. U. O.; Favre, A.; Wengel, J.; Clivio, P. *J. Am. Chem. Soc.* **2008**, *130*, 30.
(8) Douki, T. J. *Photochem. Photobiol. B: Biol.* **2006**, *82*, 45.
(9) Law, Y. K.; Azadi, J.; Crespo-Hernandez, C. E.; Olmon, E.; Kohler, B. *Biophys. J.* **2008**, *94*, 3590.
(10) Johnson, A. T.; Wiest, O. *J. Phys. Chem. B* **2007**, *111*, 14398.
(11) (a) Cohen, M. D.; Schmidt, G. M. J. *J. Chem. Soc.* **1964**, 1996. (b) Ramamurthy, V.; Venkatesan, K. *Chem. Rev.* **1987**, *87*, 433.
(12) Hariharan, M.; Lewis, F. D. *J. Am. Chem. Soc.* **2008**, *130*, 11870.
(13) (a) Kaur, H.; Arora, A.; Wengel, J.; Maiti, S. *Biochemistry* **2006**, *45*, 7347. (b) Kaur, H.; Babu, B. R.; Maiti, S. *Chem. Rev.* **2007**, *107*, 4672.
(14) Deering, R. A.; Setlow, R. B. *Biochim. Biophys. Acta* **1963**, *68*, 526.
(15) Holman, M. R.; Ito, T.; Rokita, S. E. *J. Am. Chem. Soc.* **2007**, *129*, 6.
(16) Johns, H. E.; Pearson, M. L.; LeBranc, J. C.; Helleiner, C. W. *J. Mol. Biol.* **1964**, *9*, 503.
(17) Foloppe, N.; MacKerell, A. D. *J. Comput. Chem.* **2000**, *21*, 86.
(18) Pande, V.; Nilsson, L. *Nucleic Acids Res.* **2008**, *36*, 1508.
(19) Nielsen, K. E.; Singh, S. K.; Wengel, J.; Jacobsen, J. P. *Bioconjugate Chem.* **2000**, *11*, 228.
(20) Egli, M.; Minasov, G.; Teplova, M.; Kumar, R.; Wengel, J. *Chem. Commun.* **2001**, 651.
(21) Ivanova, A.; Rosch, N. *J. Phys. Chem. A* **2007**, *111*, 9307.

JA106203Q